https://doi.org/10.5194/mr-2026-12
Preprint. Discussion started: 24 November 2026
© Author(s) 2026. CC BY 4.0 License.



Open Access MAGNETIC RESONANCE Discussions

# A practical toolbox for acquisition and processing of MAS NMR spectra obtained by heteronuclear cross relaxation under dynamic nuclear polarization (SCREAM-DNP)

Florian Philipp-Taube,[1,2] Mirjam Schröder,[1,2,3] Thomas Biedenbänder,[1,2] Edvards Roberts Bensons,[1,2] Till Biskup,[1,4] Björn Corzilius [1,2,3]

[1]Institut für Chemie, Universität Rostock, Rostock, 18059, Germany
[2]Department Life, Light & Matter, Universität Rostock, Rostock, 18059, Germany
[3]Leibniz Institute for Catalysis (LIKAT) e.V., Rostock, 18059, Germany
[4]Physikalisch-Technische Bundesanstalt, Berlin, 10587, Germany

*Correspondence to*: Florian Philipp-Taube (florian@philipp-taube.de)

**Abstract.** Dynamic nuclear polarization (DNP) significantly enhances the sensitivity of nuclear magnetic resonance (NMR) through polarization transfer from unpaired electron spins to nuclear spins. Recent developments aim at achieving site-specific signal enhancement, yet conventional approaches face challenges including paramagnetic relaxation enhancement (PRE) and the need for precise molecular positioning of paramagnetic species. Specific cross-relaxation enhancement by active motions under DNP (SCREAM-DNP) offers an alternative strategy enabling site-specificity through highly mobile functional groups. Under typical DNP conditions of 100 K, heteronuclear resonances from rapidly rotating moieties such as methyl groups appear through an indirect route via proton spin-diffusion and heteronuclear Overhauser effect in competition with direct DNP; these contributions may be separated through spectral filtering. This work provides a comprehensive overview of the entire SCREAM-DNP workflow, encompassing pulse sequence design, data acquisition and post-processing steps using Bruker TopSpin format. Furthermore, we introduce SCREAMLAB (v0.3.0), a Python package designed to enable reproducible, standardized, and transparent analysis of SCREAM-DNP data.

## 1 Introduction

Dynamic nuclear polarization (DNP) is a powerful technique within the field of nuclear magnetic resonance (NMR) spectroscopy. It substantially enhances NMR sensitivity – by several orders of magnitude – through the transfer of thermal polarization from unpaired electron spins to surrounding nuclei. In a typical experiment, a polarizing agent (PA), either a stable radical or a paramagnetic metal ion, is incorporated into the sample. Polarization transfer occurs via microwave irradiation through distinct mechanisms, including solid effect (SE), cross effect (CE), or OVERHAUSER effect (OE). When hyperpolarized nuclear spins experience homonuclear coupling in solids, spin diffusion can transport the polarization away from the PA,

https://doi.org/10.5194/mr-2026-12
Preprint. Discussion started: 24 November 2026
© Author(s) 2026. CC BY 4.0 License.



Open Access MAGNETIC RESONANCE Discussions

resulting in uniform signal enhancement throughout the entire sample.(Biedenbänder et al., 2022; Chow et al., 2022; Lilly Thankamony et al., 2017)

Recent developments in DNP have focused, among other objectives, on achieving site-specific signal enhancement – for example, to obtain structural information at particular positions of biomolecules or materials.(Busch et al., 2025) Specificity can be achieved through several approaches, such as covalent attachment of paramagnetic species to the molecule of interest or functionalization of molecules with paramagnetic moieties designed to bind selectively to target proteins.(van der Cruijsen et al., 2015; Goldfarb, 2014; Heiliger et al., 2020; Herr et al., 2021; Kaushik et al., 2016; Klug and Feix, 2008; Marin-Montesinos et al., 2019; Rogawski et al., 2017; Viennet et al., 2016; Voinov et al., 2015) For membrane proteins, an effective strategy involves direct attachment of the spin label to membrane lipids, thereby generating a uniformly labeled membrane system.(Good et al., 2019; Smith et al., 2015) A general challenge common to all these methods is paramagnetic relaxation enhancement (PRE).(van der Cruijsen et al., 2015; Heiliger et al., 2020; Marin-Montesinos et al., 2019; Rogawski et al., 2017; Viennet et al., 2016) Nuclei residing within a defined sphere surrounding the paramagnetic species undergo accelerated relaxation, leading to significant line broadening. In severe cases, resonance signals may become too broadened for detection. SCREAM-DNP, first described by DAUBE et al. in 2016,(Daube et al., 2016) offers an alternative to achieve site-specificity in DNP-enhanced NMR experiments and has demonstrated efficacy in diverse biomolecular research questions.(Aladin et al., 2019, 2023; Daube et al., 2019; Mao et al., 2019) SCREAM-DNP enables homogeneous distribution of the paramagnetic species within the sample while generating specificity through the presence of a highly mobile functional group. It manifests itself within direct polarization (DP) spectra of a heteronuclear species (X) subject to time-dependent dipolar coupling to protons (H). Here, it can be observed that resonances of specific functional groups providing pronounced mobility under typical DNP conditions (100 K) appear with additionally enhanced signal intensities, and, in the case of heteronuclei with a positive gyromagnetic ratio, inverted phase (i.e., emissive lineshape). Examples of such motions include methyl group rotations, ring puckering motions,(Aladin and Corzilius, 2019; Hoffmann et al., 2017) or the dynamics of ammonium groups,(Park et al., 2020) where in the latter example the additional enhancement is positive due to $^{15}$N's negative gyromagnetic ratio.

The origin of these additional signal intensities lies in the different polarization transfer pathways from the electron to the nucleus of interest under continuous microwave irradiation. Given the DNP matching condition is chosen to allow for positive CE of all nuclear spin species, the direct DNP pathway mediated by the hyperfine interaction between electron and heteronucleus (Figure 1) results in positive signal enhancement. In the additional indirect pathway, protons of the matrix are first hyperpolarized and the polarization is then spread to protons attached to the dynamical functional group of interest via spin-diffusion (SD). From there, the polarization is transferred spontaneously to the nuclei of interest via heteronuclear Overhauser effect (hetNOE) resulting in the cross relaxation (CR) signal enhancement according to $\varepsilon_{\mathrm{CR}} = 1 - (\varepsilon_{\mathrm{H}} - 1)\frac{\gamma_{\mathrm{H}}}{\gamma_{\mathrm{X}}}\frac{\sigma_{\mathrm{HC}}}{\rho_{\mathrm{X}}}$.(Daube et al., 2019) The hetNOE itself is just active when there are fluctuations in the local magnetic field in the surrounding of the nucleus of interest. From the receiving nucleus, however, it is possible that polarization

https://doi.org/10.5194/mr-2026-12
Preprint. Discussion started: 24 November 2026
© Author(s) 2026. CC BY 4.0 License.



Open Access MAGNETIC RESONANCE Discussions

spreads in the heteronuclear network via proton-driven spin diffusion (PDSD) or it can be selectively transferred via rotational resonance.(Biedenbänder et al., 2023)

To achieve site specificity, only the indirect pathway is of interest since it only contains the resonances corresponding to mobile functional groups or atoms in their vicinity. The isolation of the indirect pathway is challenging but can be done using a pulse sequence involving proton saturation during polarization build-up, as is discussed in more detail below.

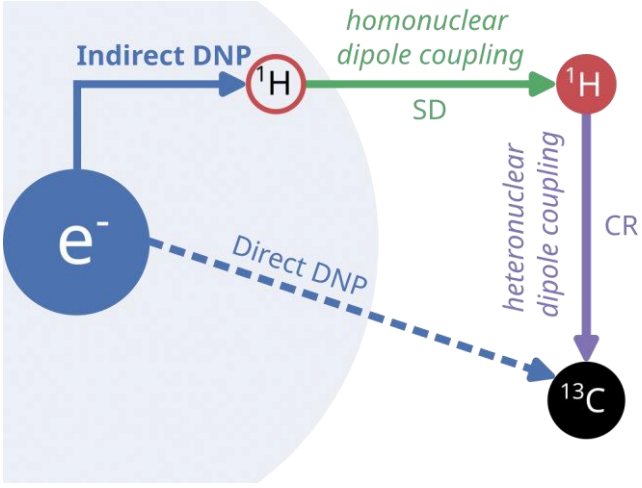


**Figure 1: Illustration of the direct and indirect DNP pathways.**

## 2 Results and Discussion

### 2.1 SCREAM-DNP pulse sequence

The main challenge of SCREAM-DNP lies in isolating the contribution of the indirect pathway ($\Delta DP_{sat}$) which cannot be measured directly but can be obtained by subtracting two spectra. The first is a conventional direct polarization (DP) spectrum, in which both the direct and indirect polarization pathways are active. The second, referred to as the $DP_{sat}$ spectrum, is recorded under similar conditions as the DP spectrum except that $\pi$ pulses are continually applied to the proton channel during the polarization buildup period, preventing buildup of proton polarization and effectively suppressing the indirect pathway. Subtracting the $DP_{sat}$ spectrum from the DP spectrum then yields a difference spectrum containing only the contribution from the indirect polarization transfer pathway ($\Delta DP_{sat}$).

In order to avoid any artifacts due to drifts in temperature etc., the pulse sequence (Figure 2) consists of two interleaved acquisition blocks. To provide better reproducibility, in both blocks the $^1$H and X spins' magnetizations are fully quenched prior to the polarization buildup period by a 90°-pulse train. In the pulse sequence (Supporting Information) this is implemented by a pulse of duration P1 at power level PLW1 on the heteronucleus as well as P4 at power level PLW3 on $^1$H, followed by a delay D4; these saturation pulses are looped L4 times. Pulse powers and durations can be simply set to a 90°-pulse, however, slightly larger pulse angles may improve saturation efficiency. D4 and L4, however, have to be chosen according to the

https://doi.org/10.5194/mr-2026-12
Preprint. Discussion started: 24 November 2026
© Author(s) 2026. CC BY 4.0 License.

Open Access MAGNETIC RESONANCE Discussions

relaxation properties of the sample: D4 must be long enough to allow for complete dephasing of transverse magnetization, but short enough to prevent partial longitudinal relaxation while L4 must be set large enough to achieve a quasi-stationary saturation state. In our experience, D4 = 5 ms and L4 = 16 turned out to be a robust choice for $^{13}C$ in amino acids.

Spectra are then recorded by single-pulse excitation (Bloch decay) under standard proton decoupling after a polarization buildup period ($t_{pol}$). The polarization buildup time may be varied by incrementing the number of repeat units (L20) of equally long periods (D20). Each repeat unit contains one 180° pulse with a pulse duration of P20 and a delay of D20 so that the total polarization buildup time is $t_{pol} = L20 \cdot (P20 + D20)$. However, since D20 is typically in the range of a few hundred milliseconds while a pulse duration is typically a few microseconds, the pulse length can be neglected in first approximation resulting in $t_{pol} = L20 \cdot D20$. In the first block, no $^{1}H$ saturation is applied, i.e., the corresponding pulse power (PLW21) is set to 0 W. Thus, the direct polarization (DP) spectrum is obtained. During the second block, all $^{1}H$ spin magnetization is continually inverted by setting the corresponding pulse power (PLW20) to a value corresponding to a 180° pulse. As all other conditions are equal, this results in the $DP_{sat}$ spectrum that ideally only contains contributions from the direct DNP transfer pathway. Free induction decays (FIDs) are stored in a pseudo-2D format where the first slice belongs to the DP spectrum and the second slice to the $DP_{sat}$ spectrum. Numerical subtraction yields the $\Delta DP_{sat}$ spectrum, which shows only the magnetization transferred via the CR-induced indirect pathway; this step will be discussed in more detail later. Note that D20 must be chosen significantly shorter than the $T_1$ of $^{1}H$ in order to allow for an effective saturation of the $^{1}H$ polarization. Shorter D20 periods improve saturation efficiency, but increase the pulse duty cycle during the up to hundreds of seconds long polarization buildup period. Longer D20 approaching the $T_1$ of $^{1}H$ reduce the fidelity of the saturation filter and thus the signal amplitude of the $\Delta DP_{sat}$ spectra, but do not introduce any artifacts. In most cases under DNP conditions, $T_1$ is in the order of a few seconds so D20 = 0.25 s serves as a good starting point; in this case, the duty cycle is on the order of 20 ppm or lower, resulting in a negligible power load in the radio frequency circuit of below 1 mW during the buildup under proton saturation.

A practical strategy to extract the SCREAM-DNP buildup time constants is to vary $t_{pol}$ by exponentially incrementing L20, for example, as a power of base two or square root of two, starting from short polarization times, for example 0.25 s, up to longer times such as 64 s, although the exact range depends on the system under study. Note that D20 marks the lower limit for $t_{pol}$. Also, for polarization times shorter than 1 s (assuming a max. 50 ms long acquisition/decoupling window), an interscan delay (D1) of, e.g., 1 s ensures proper overall duty cycle, whereas for longer polarization times, D1 can be reduced to e.g. 0.1 s for overall time savings. Since experimental time increases with polarization time, it is efficient to use a higher number of scans for short polarization times and fewer scans for longer periods in which case spectra must be normalized to the number of scans for proper buildup parameter extraction; as will be explained below, SCREAMLAB will automatically take care of this task.

https://doi.org/10.5194/mr-2026-12
Preprint. Discussion started: 24 November 2026
© Author(s) 2026. CC BY 4.0 License.

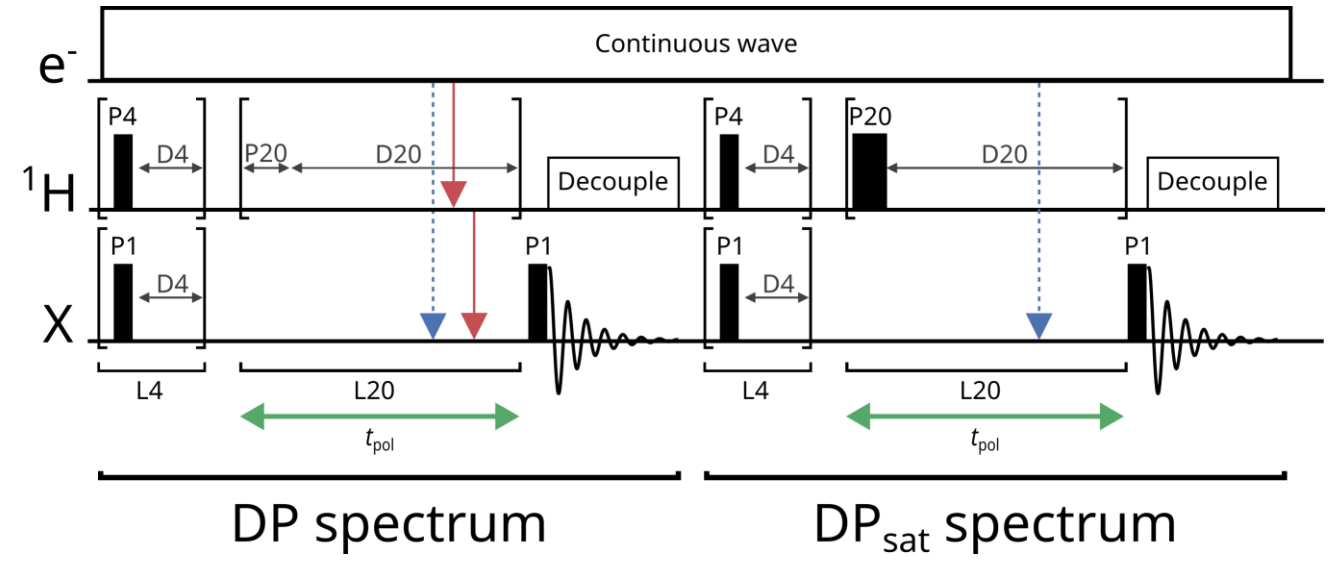


**Figure 2. SCREAM-DNP pulse sequence showing two DP acquisitions one with and one without proton saturation resulting in the DP and $DP_{sat}$ spectra. Direct DNP pathway and indirect CR based transfer pathways are indicated with blue (dotted line) and red (solid line) arrows, respectively. Delays (D), pulse durations (P), and loops (L) are defined as implemented in the pulse sequence (see Supporting Information). In the DP spectrum, P20 serves as a placeholder and the corresponding radio frequency power is set to 0 W, so no pulse is applied. In the $DP_{sat}$ spectrum, by contrast, P20 is an active pulse and is applied. Note that the recycle delay is not shown in this scheme.**

### 2.2 Post-processing of spectra

The post-processing of SCREAM-DNP spectra involves several steps. To facilitate this, we provide the Jython script "scream.py" (Supplementary Material), which can be integrated into the TopSpin command library (e.g. via the TopSpin command "edpy"). Execution of "scream" from the TopSpin command line initiates the processing of a SCREAM-DNP spectrum.

The resulting spectra are saved under the same experiment number (expno), but with distinct processing number (procno) identifiers: procno 101 contains the DP spectrum, while procno 102 corresponds to the $DP_{sat}$ spectrum. The $\Delta DP_{sat}$ spectrum which may exhibit either positive or negative signals, depending on the gyromagnetic ratio of the heteronucleus, is saved under procno 103.

If necessary, processing steps such as phase correction, baseline correction, and related adjustments can be applied. To ensure consistency in the processing parameters across the three spectra (DP, $DP_{sat}$, and $\Delta DP_{sat}$), we recommend optimizing these parameters on either the $DP_{sat}$ or the $\Delta DP_{sat}$ spectrum, subsequently transferring them to the pseudo-2D experiment (procno = 1), and rerunning the "scream" command. For kinetic series measurements (e.g., polarization buildup series), it is advisable to maintain identical processing parameters across all experiments with varying polarization times, provided that the acquisition parameters are uniform and the interval between experiments is sufficiently short.

https://doi.org/10.5194/mr-2026-12
Preprint. Discussion started: 24 November 2026
© Author(s) 2026. CC BY 4.0 License.

Open Access MAGNETIC RESONANCE Discussions

### 2.3 Data Analysis

#### 2.3.1 General process

The most commonly used approach for analyzing SCREAM-DNP data involves the evaluation of CR buildup times or buildup rate constants. The extraction of these parameters from post-processed spectra follows the workflow illustrated in Figure 3. We will first give a brief overview of the whole process, before going into much more detail in the following sections. After importing the spectral data into the SCREAMLAB environment, the first step involves extracting intensity values for each polarization time. This can be accomplished using various methods. The simplest approach employs the numerical integration (later called "numint") of spectral data points within a specified range as the intensity metric. This approach becomes problematic in the presence of overlapping spectral signals. For such cases, an alternative strategy involves deconvolving the individual signals, numerically integrating each fitted component separately using the resulting integral as the intensity metric. Note that while the amplitude parameters of the deconvolution functions could also serve as an intensity metric, we used numerical integration, consistent with the workflow implemented for "numint". Peak profiles may be modeled using a GAUSS function, a LORENTZ function, or a VOIGT profile combining both functional forms, with the choice depending on the relative contributions of homogeneous and inhomogeneous line broadening in the spectrum.

Spectral deconvolution can be performed using two distinct approaches. First, each peak in each spectrum can be fitted to an individual set of parameters, including the peak center, line broadening parameters, and peak amplitude. This approach will subsequently be termed "individual". The second approach assumes that the peak center and the line broadening parameter for each peak remain constant across all spectra, while only the peak amplitude varies with polarization time. This approach will subsequently be termed "global".

Regardless of which fitting strategy is employed, the procedure yields a dataset comprising paired values of polarization time and corresponding intensity. From this dataset, the buildup time constants or buildup rate constants can subsequently be extracted via least-square fitting of exponential, biexponential, or stretched-exponential functions which are ideally constrained to pass through the origin, assuming the saturation pulse trains applied prior to measurement ensure that no net polarization exists on the target nuclei at time zero.

The analysis concludes with the generation of a comprehensive report containing the extracted kinetic parameters along with associated fitting parameters.

https://doi.org/10.5194/mr-2026-12
Preprint. Discussion started: 24 November 2026
© Author(s) 2026. CC BY 4.0 License.



Open Access MAGNETIC RESONANCE Discussions

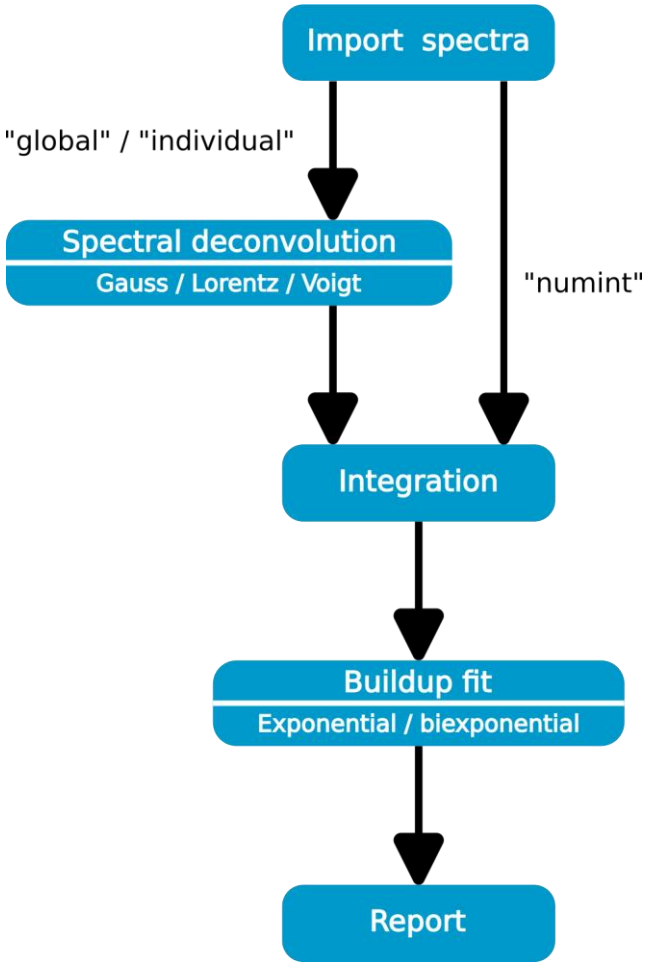


**Figure 3. Schematic representation of steps performed during one analysis with SCREAMLAB starting with the import of a spectrum followed by the spectral deconvolution, integration and buildup analysis.**

### 2.3.2 Implementation

The package is implemented in Python following best practices of scientific software development.(Biskup, 2026) It is written object-oriented and was developed with high test coverage to ensure correct behavior at the time of development and later upon extension and refactoring. The testing process is automated using the Python unit testing framework. Code quality is improved using an automatic code formatter, Black,(Langa, 2018) together with Prospector for static code analysis.(Prospector Development Team, n.d.) The documentation is incorporated into the code itself, and additional concepts and examples of usage are documented alongside the code. The automated documentation formatting tool, Sphinx,(Sphinx Development Team, 2026) transforms the documentation into HTML pages, which are available online on https://screamlab.readthedocs.io/en/latest/. The software is released under a permissive license (BSD 2-Clause) and is available

https://doi.org/10.5194/mr-2026-12
Preprint. Discussion started: 24 November 2026
© Author(s) 2026. CC BY 4.0 License.

Open Access MAGNETIC RESONANCE Discussions

for installation from Python Packaging Index (PyPI). The source code is published on Zenodo,(Taube, 2026) which ensures long-term availability and offers possibility for citation due to the inclusion of a Digital Object Identifier.

### 2.3.3 Setting properties

In the following part we will present possible options on how to use the package and give examples of successful application to real datasets. The Python package comprises two core classes: PROPERTIES, which encapsulates all configurable parameters, and DATASET, responsible for storing experimental data and managing associated processing and analysis operations. The initialization procedure begins with the instantiation of the PROPERTIES class, followed by specification of the experiment directory and assignment of experiment numbers (expno) as a list (see Scheme 1). Note that a minimum of four spectra acquired at different polarization times is required. Experiment number input is supported via two alternative ways. First, a two-element list may be provided, interpreted as a “from-to” range; second, an explicit list containing four or more individual experiment numbers can be supplied directly. In its default configuration, the framework locates $\Delta DP_{sat}$ spectra at procno 103 per experiment, matching the output convention of the “scream.py” post-processing script discussed above. This parameter can be reconfigured manually to accommodate alternative data storage schemes or, e.g., to analyze the $DP_{sat}$ spectra instead. For the intensity metric determination the preferred method must be specified at this point. Per default, a “global” fit will be performed, however, also “individual” or “numint” are valid options. Output configuration allows specification of a target directory for generated result files. When the specified path (/path/to/output_folder) does not exist, the framework automatically creates the corresponding directory. An implementation of the procedure described above is provided below:

```
from screamlab import settings, dataset


properties = settings.Properties() #Instantiation of PROPERTIES class
properties.path_to_experiment = r"/path/to/dataset" #Specification of experiment directory
properties.expno = [1, 8] #Assignment of experiment numbers
properties.procno = 102 #Default value: 103; optional
properties.output_folder = r"/path/to/output_folder" #Specification of output directory
properties.spectrum_fit_type = “global” #”Default: “global”, “individual”, “numint” possible
```

In the next step, the DATASET object must be instantiated and configured by assigning an instance of the previously described PROPERTIES class to its properties attribute as follows:

```
dataset = dataset.Dataset() #Instantiation of DATASET class
dataset.properties = properties #Pass properties class
```

https://doi.org/10.5194/mr-2026-12
Preprint. Discussion started: 24 November 2026
© Author(s) 2026. CC BY 4.0 License.

Open Access MAGNETIC RESONANCE Discussions

### 2.3.4 Spectral deconvolution

Spectral deconvolution and determination of dynamic parameters require identification of peak positions. The function dataset.add_peak() adds a single peak to DATASET by specifying its center position with an accuracy of ±1 ppm. Note, this step must be done either manually or in combination with automatic peak picking methods like find_peaks() from SciPy. Optional arguments include a descriptive label (default: "Peak_at_xxx_ppm"), the peak signature (default: "-"), and additional parameters addressed subsequently. If the "numint" approach is to be employed, the integration range must be specified at this stage by providing a list containing two float values. Several examples demonstrating the use of the dataset.add_peak() function described above are provided in the following lines of code.

```
# Negative peak at -16.5 ppm, labeled Peak_at_m16_ppm.
dataset.add_peak(-16.5)

# Positive peak at 12 ppm, labeled Peak_at_12_ppm.
dataset.add_peak(12, peak_sign="+")

# Positive peak at 2.5 ppm, labeled C_alpha.
dataset.add_peak(2.5, peak_sign="+", peak_label="C_alpha")

# Negative peak at -5 ppm, labeled C_beta.
dataset.add_peak(-5, peak_label="C_beta")

# Negative peak at -5 ppm, labeled C_beta. Numerical integration of peak between 0 and -10 # ppm if dataset.properties.spectrum_fit_type = "numint"
dataset.add_peak(-5, peak_label="C_beta", integration_range = [0, -10])
```

With these specifications in place, the workflow can be initiated by calling the dataset.start() function. During the data loading – which relies on the Python package nmrglue(Helmus and Jaroniec, 2013) – *x*- and *y*-axes of all spectra are imported and the polarization time of each spectrum is automatically calculated from the delay (D20) and the loop counter (L20). The spectral intensities are automatically normalized to the number of scans used during acquisition. This allows the experimentalist to optimize the measurement time: experiments at shorter polarization times may utilize higher number of scans, while those as extended polarization times may employ fewer scans, thereby maximizing the signal-to-noise ratio (SNR) for all experiments globally.

In the standard configuration, each spectral resonance is modeled using a VOIGT lineshape profile:

$$f(x, A, \mu, \sigma, \gamma) = \frac{A\mathrm{Re}[w(z)]}{\sigma\sqrt{2\pi}} \quad (1)$$

https://doi.org/10.5194/mr-2026-12
Preprint. Discussion started: 24 November 2026
© Author(s) 2026. CC BY 4.0 License.



Open Access MAGNETIC RESONANCE Discussions

With

$$z = \frac{x - \mu + i\gamma}{\sigma * \sqrt{2}} \tag{2}$$

where $\sigma$ and $\gamma$ represent the GAUSS and LORENTZ line broadening parameters, $\mu$ and $A$ denote the center and amplitude of the signal, respectively. $w(z)$ is the FADDEEVA function.(Olver et al., 2026) Note that if "numint" is selected, this entire spectral deconvolution step does not apply.

Based on these specifications, the spectrum is fitted to one VOIGT lineshape or to a sum of VOIGT lineshapes. The entire fitting process is based on the minimize() function provided by the Python package LMFIT (v1.3.1).(Newville et al., 2014) Different configuration options are available during this procedure:

1. By default, the two VOIGT lineshape parameters, $\sigma$ and $\gamma$, are allowed to vary between 0 ppm and 3 ppm. However, if the signal exhibits a broader linewidth or if more precise parameters are already known, the default range for line broadening can be adjusted in the dataset.add_peak() function.

```
# Negative peak at -5 ppm, label: ”Peak_at_m5_ppm”. Sigma is allowed to vary
# between two and for and gamma between 1 and 5 during deconvolution.
lb = {“sigma”: {“min” : 2,”max : 4”}, “gamma”:{“min” : 1,”max : 5”}}
dataset.add_peak(-5, line_broadening = lb)

# Negative peak at -5 ppm, label: “Peak_at_m5_ppm”. Sigma is allowed to vary
# between two and for and gamma stays at the default values.
lb = {“sigma”: {“min”: 2,”max : 4”}}
dataset.add_peak(-5, line_broadening = lb)
```

2. In some cases, resonances can be modeled using simpler lineshapes than the VOIGT profile. For these instances, it is also possible to simulate a signal with a GAUSS

$$f(x, A, \mu, \sigma) = \frac{A}{\sigma\sqrt{2\pi}} \cdot e^{-\frac{(x-\mu)^2}{2\sigma^2}} \tag{3}$$

or LORENTZ lineshape

$$f(x, A, \mu, \gamma) = \frac{A}{\pi} \cdot \frac{\gamma}{(x-\mu)^2 + \gamma^2} \tag{4}$$

with the same definition of symbols as above (Figure 4).

https://doi.org/10.5194/mr-2026-12
Preprint. Discussion started: 24 November 2026
© Author(s) 2026. CC BY 4.0 License.

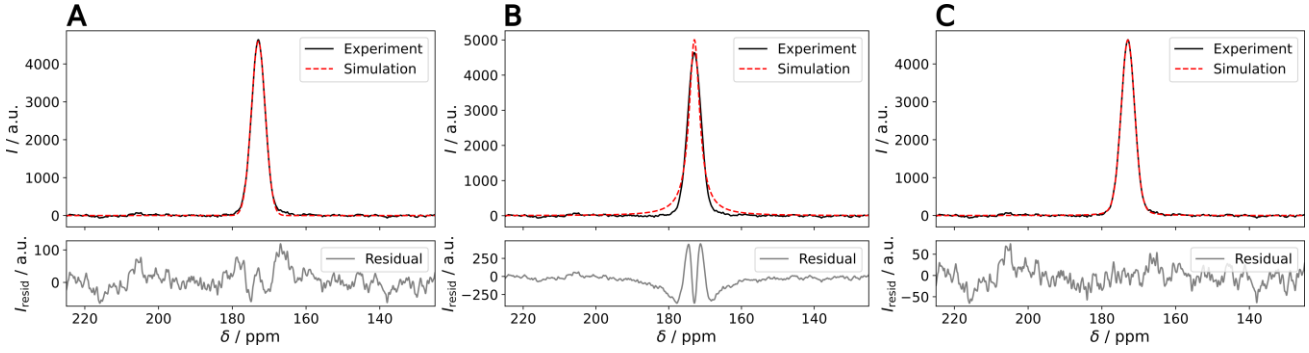


**Figure 4. Example representation of three identical peaks corresponding to the carbonyl carbon of $^{13}$C-L-alanine (0.2 M) in DNP matrix containing 2.5 mM AMUPol, fitted using (A) a GAUSS, (B) a LORENTZ, and (C) a VOIGT profile. The comparison demonstrates that a GAUSS function provides a sufficiently accurate fit for the data, despite the Voigt profile offering a marginally better representation, particularly in the regions of the peak tails. The LORENTZ profile fails to adequately capture the peak shape and is therefore not suitable for this dataset. Details about the experimental data underlying this study are provided in the Supporting Information. Note that the signal was inverted for sake of simplicity.**

The lineshape can be changed in the add_peak() function of each signal and the customization of line broadening parameters proceeds analogously to the procedure previously described. Note that applying an exponential window function prior to FOURIER transform inherently introduces a LORENTZ line broadening component to the spectral signal.

```
# Negative peak at -5 ppm, labeled Peak_at_m5_ppm. Peak is described
# via a GAUSS  distribution
dataset.add_peak(-5, fitting_type="gauss")   #"voigt", "lorentz"
```

3. A preliminary fit (prefit) can be performed on one spectrum to obtain an initial estimation of the peak parameters. If a prefit is performed, it is assumed for all subsequent steps that the linewidth parameters may vary within a range of ± 10 % from the values determined by the prefit. By default, the spectrum used for the prefit is the last entry in the properties.expno list since it often has the best signal to noise ratio. The execution of the prefit procedure as well as the selection of the spectrum for the prefit can be specified via the PROPERTIES class:

```
properties.prefit = True                          #Default: False
properties.spectrum_for_prefit = 4  #Fourth element in properties.expno. Default: -1 meaning the last element
#corresponding to the spectrum with the longest buildup time
```

4. To reduce computation time during spectral deconvolution, the spectrum may be divided into distinct regions for independent fitting (Figure 5). Despite this optimization, calculation times ranging from minutes to hours remain possible, depending on the number of resonances per spectrum, the number of spectra and the selected fitting approach. The subspectra can be specified via the PROPERTIES class. Note, for each subspectrum, dataset.start() must be called again

https://doi.org/10.5194/mr-2026-12
Preprint. Discussion started: 24 November 2026
© Author(s) 2026. CC BY 4.0 License.

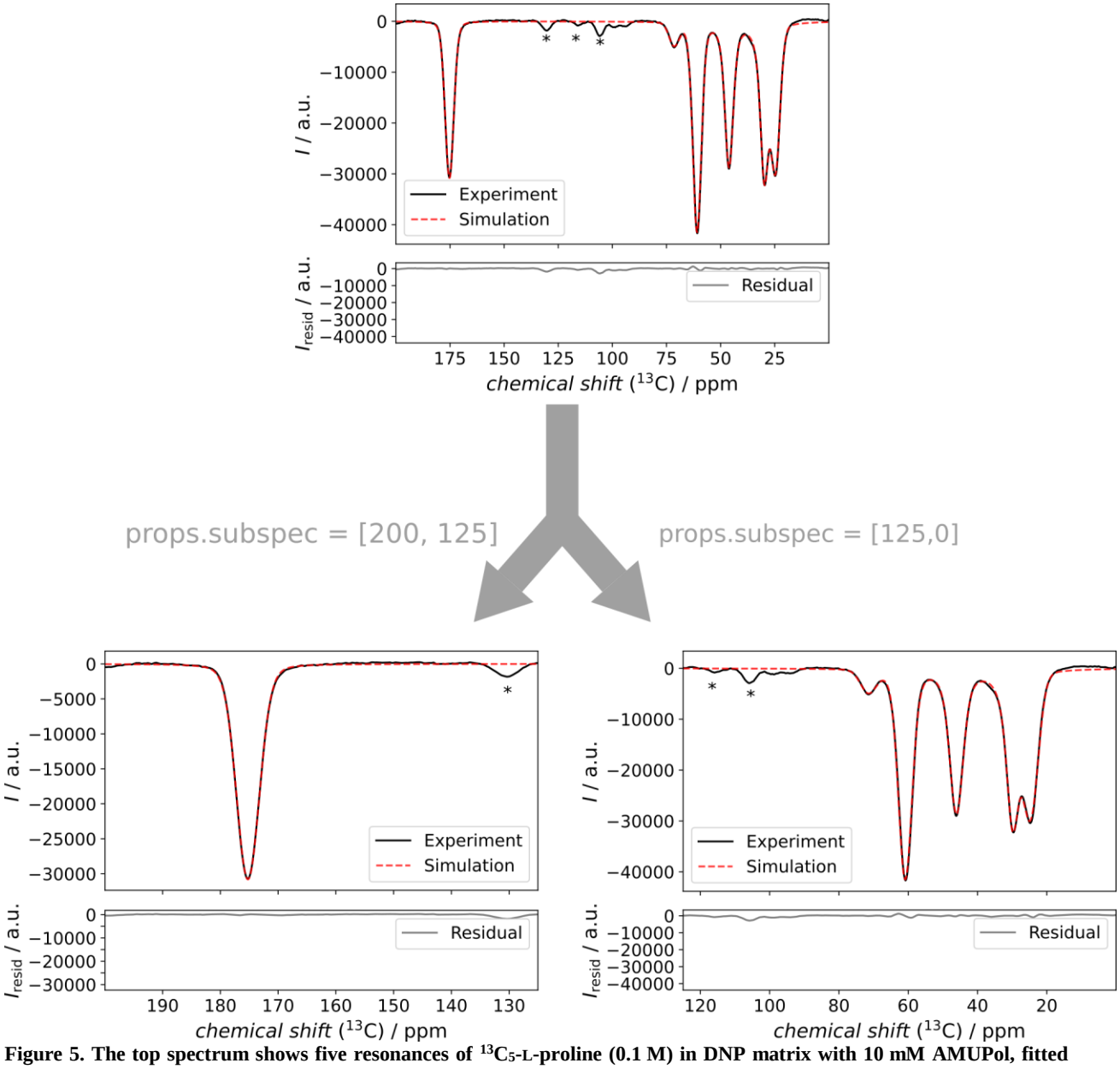


**Figure 5. The top spectrum shows five resonances of $^{13}C_5$-L-proline (0.1 M) in DNP matrix with 10 mM AMUPol, fitted simultaneously. Note that besides the 5 proline resonances at 175 ppm (Carbonyl), 61 ppm (Cα), 46 ppm (Cδ), 30 ppm (Cβ) and 25 ppm (Cγ) an additional resonance appears at 71 ppm which belongs to glycerol. The second glycerol signal overlaps with the Cα resonance of proline. Rotational sidebands are markted with an asterisk. In the lower panel, the spectrum is split into two subspectra (properties.subspec = [200, 125] and properties.subspec = [125, 0]): one with a single resonance fitted independently, and another with the remaining four. This *subspec* approach reduces computational time by minimizing the number of parameters optimized at once. Spectra are recorded at 100 K, 8 kHz MAS frequency and with a polarization time of 128 s. Details about the experimental data underlying this study are provided in the Supporting Information and data are available at Zenodo (https://zenodo.org/records/24086268).**

https://doi.org/10.5194/mr-2026-12
Preprint. Discussion started: 24 November 2026
© Author(s) 2026. CC BY 4.0 License.

Open Access MAGNETIC RESONANCE Discussions

Following spectral deconvolution, SCREAMLAB automatically integrates the simulated signals and assigns the intensity metrics to the corresponding polarization times. In the case of "numint" approach, the deconvolution step is omitted, and the peak ranges are integrated directly. The framework then proceeds directly to evaluate dynamic parameters without manual intervention.

### 2.3.5 Evaluation of dynamic parameters

In the simplest case, the polarization buildup can be described using an exponential function:

$$I(t_{\mathrm{pol}}) = A_{\mathrm{f}}\left(1 - e^{-t_{\mathrm{pol}}/t_{\mathrm{f}}}\right) \tag{5}$$

where $A_{\mathrm{f}}$ represents the maximum SCREAM-DNP signal intensity virtually reached at infinitely long polarization time and $t_{\mathrm{f}}$ represents the CR buildup time constant. This functional form guarantees that $I(t_{\mathrm{pol}} = 0) = 0$, which is, as mentioned above, a necessary condition since the polarization process begins immediately following saturation pulses that nullify the total magnetization of both protons and heteroatoms. The output explicitly provides both, the buildup time constant $t_{\mathrm{f}}$ and its inverse, the buildup rate constant $R_{\mathrm{f}} = 1/t_{\mathrm{f}}$. By default, SCREAMLAB employs this model for fitting, though alternative functions are available.

A frequently observed phenomenon in SCREAM-DNP experiments is biexponential buildup behavior, characterized by fast and slow processes. Empirically, the fast component can be assigned to the hetNOE/SCREAM-DNP, while the physical origin of the slow process remains incompletely understood.(Aladin and Corzilius, 2019; Biedenbänder et al., 2023; Daube et al., 2016; Taube et al., 2026) In this case, the buildup kinetics are described as:

$$I(t_{\mathrm{pol}}) = A_{\mathrm{f}}\left(1 - e^{-t_{\mathrm{pol}}/t_{\mathrm{f}}}\right) + A_{\mathrm{s}}\left(1 - e^{-t_{\mathrm{pol}}/t_{\mathrm{s}}}\right) \tag{6}$$

where $t_{\mathrm{f}}$ and $t_{\mathrm{s}}$ are the fast and slow buildup times, respectively, and the maximum SCREAM-DNP signal intensity at infinitely long polarization time can be described as $A_{\mathrm{max}} = A_{\mathrm{f}} + A_{\mathrm{s}}$. In addition to the two functions typically used, several supplementary functions addressing more specialized cases are provided. Details are given in the documentation.

Plots of signal intensity versus time are again fitted using the minimize() function implemented in LMFIT (version 1.3.1) (Newville et al., 2014) In the default configuration, buildup time constants were constrained to vary within the range from zero to three times the maximum polarization duration. Similarly, the amplitude parameters for positive or negative signals were allowed to vary between zero and three times the maximum or minimum signal intensity, respectively.

To enhance fit quality and reduce dependence on initial parameter estimates, the fitting procedure is iterated $n \cdot 50$ times, where $n$ denotes the number of fitting variables. Each iteration employed distinct initial conditions for all free parameters, generated using Latin Hypercube Sampling (LHS) – a near-random sampling approach that efficiently explores the multidimensional parameter space.(McKay et al., 1979) The implementation of LHS functions relied on the Python package PYDOE3.(Lafage et al., 2023) Among the resulting replicas, the optimal simulation is selected based on the lowest χ-squared statistic.

https://doi.org/10.5194/mr-2026-12
Preprint. Discussion started: 24 November 2026
© Author(s) 2026. CC BY 4.0 License.

Open Access MAGNETIC RESONANCE Discussions

### 2.3.6 Output

As scientific research data should follow the FAIR principles (findable, accessible, interoperable, reusable),(Wilkinson et al., 2016) our implementation is designed to maintain a fully traceable and well-documented data processing workflow. All options, parameters, functions, and procedural steps are explicitly recorded throughout each stage of analysis ensuring that results can be independently verified and reproduced.

The primary output is a structured text file named "analysis_result.txt", which systematically documents all information generated during the pipeline in five sections:

1. Overview of configuration settings defined in the PROPERTIES class, including default values and metadata on the number of peaks and spectra processed.
2. Information for each fitted peak, including: center position, label, lineshape function selected for the deconvolution, sign assignment, and the parameter boundaries used as constraints during the fitting procedure.
3. Results from prefit for each individual peak, if prefit was performed.
4. Results of the spectral deconvolution stage presenting all fitting result parameters along with additional derived values.
5. Results of the buildup dynamic fitting stage presenting all fitting result parameters along with additional derived values.

In cases of "global" and "individual" fitting approach, the additional entries include the full width at half maximum (FWHM, $\Delta$ in ppm) for GAUSS, LORENTZ, and/or VOIGT lineshapes as well as the integral area of each peak. The FWHM is calculated using

$$\Delta_{\text{Gauss}} = 2 \cdot \sqrt{2\ln(2)} \cdot \sigma \tag{7}$$

for GAUSS,

$$\Delta_{\text{Lorentz}} = 2\gamma \tag{8}$$

for LORENTZ, and

$$\Delta_{\text{Voigt}} \approx 0.5346\Delta_{\text{Lorentz}} + \sqrt{0.2166\Delta_{\text{Lorentz}}^2 + \Delta_{\text{Gauss}}^2} \tag{9}$$

for VOIGT where $\sigma$ and $\gamma$ represent the line broadening parameters derived from the best fit.

In cases of buildup time constant determination, as additional parameter, the time-weighted intensity $\Sigma$ is calculated as follows:

$$\Sigma_i = \frac{A_i}{\sqrt{t_i}} \tag{10}$$

where $i$ represents the fast or slow buildup process, with $A_i$ being the respective plateau intensities and $t_i$ the buildup time constant.

Several folders are automatically generated, each containing graphical representations or more precise information. The "buildup_plots" and "spectral_deconvolution_plots" folders contain graphical representations of fitting results in multiple file

https://doi.org/10.5194/mr-2026-12
Preprint. Discussion started: 24 November 2026
© Author(s) 2026. CC BY 4.0 License.

Open Access MAGNETIC RESONANCE Discussions

formats (PDF and PNG). The "spectra" folder contains a CSV file with the raw spectral data points, along with a graphical representation of the spectra. These were imported from TopSpin to SCREAMLAB and normalized to the number of scans. Since all fitting within SCREAMLAB is performed using the Python package LMFIT (v1.3.1), the original LMFIT result files – including additional fitting information such as fitting statistics and correlations between the parameters – are saved in the "lmfit_reports" folder. Additionally, the values obtained from the fitting process are provided in a semicolon-separated table in the "tabular_results" folder, designed to facilitate easy incorporation of the results into supporting materials for publications or for further usage in Python or other programs/programming languages.

```
output_folder
├── analysis_report.txt
├── buildup_plots
├── lmfit_reports
├── spectra
├── spectral_deconvolution_plots
└── tabular_results
```

### 2.4 Working with SCREAMLAB

To illustrate the practical application of SCREAMLAB, this section presents a detailed case study. In this example, we analyze a 0.1 M frozen solution of $^{13}C$,$^{15}N$-L-Pro in DNP matrix (glycerol-$d_8$:$D_2O$:$H_2O$, 60:30:10 vol-%), containing 10 mM AMUPol as polarization agent. SCREAM-DNP spectra were acquired with polarization times ranging from 1 s to 512 s. The code presented below aims for a global fit across all five proline resonances over all polarization times, followed by an exponential and biexponential dynamic evaluation.

```
from screamlab import settings, dataset

properties = settings.Properties()
properties.path_to_experiment=r'..\path\to\experiments'
properties.expno = [1,10]
properties.prefit = True
properties.spectrum_for_prefit = -1
properties.buildup_types = ["exponential", "biexponential"]
properties.output_folder = r'path/to/output_folder'

ds = dataset.Dataset()
```

https://doi.org/10.5194/mr-2026-12
Preprint. Discussion started: 24 November 2026
© Author(s) 2026. CC BY 4.0 License.



```
ds.props = properties


ds.add_peak(175, peak_sign='-' , fitting_type="voigt", peak_label="Carbonyl_C")
ds.add_peak(71, peak_sign='-' , fitting_type="gauss", peak_label="Glycerol_C2"
ds.add_peak(61, peak_sign='-' , fitting_type="voigt", peak_label="Calpha_and_glycerol")
ds.add_peak(46, peak_sign='-' , fitting_type="voigt", peak_label="Cdelta")
ds.add_peak(30, peak_sign='-' , fitting_type="voigt", peak_label="Cbeta")
ds.add_peak(25, peak_sign='-' , fitting_type="voigt", peak_label="Cgamma")
ds.start_analysis()
```

As shown, all five resonances are fitted to a VOIGT lineshape. A prefit is performed on the spectrum with the highest polarization time (default setting). As clearly demonstrated in Figure 6, a biexponential buildup is needed to properly describe the polarization buildup, revealing fast and slow buildup components with buildup time constants of approximately 15 s and 150 s, respectively, for all five resonances. The full dataset as well as the full analysis report can be found in the Supporting Information.

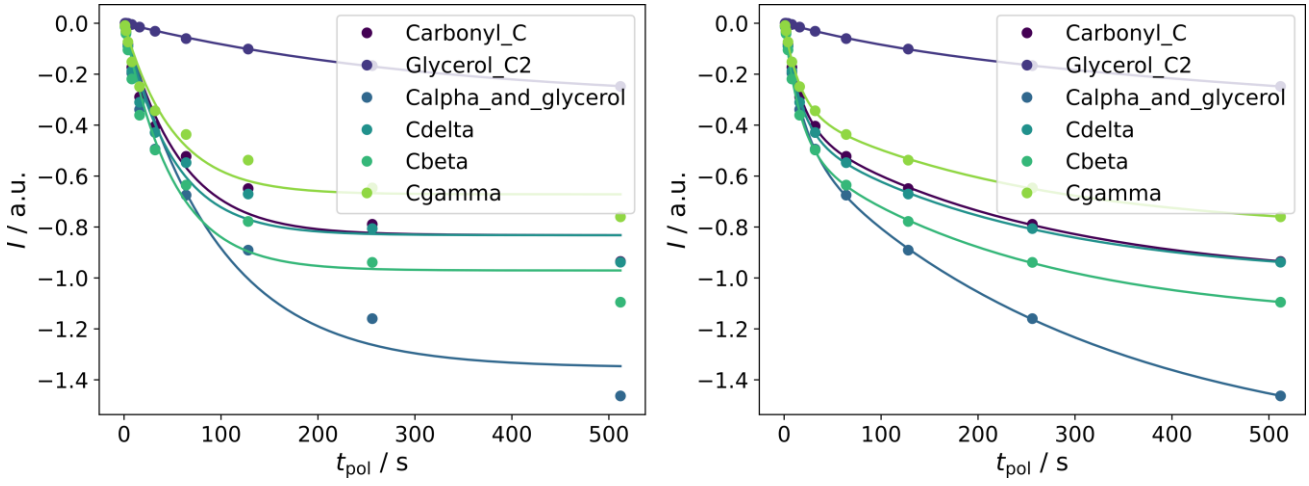


**Figure 6. SCREAM-DNP polarization buildup of 0.1 M $^{13}C_5$-L-proline in DNP juice containing 10 mM AMUpol at 100 K and 8 kHz MAS frequency. The polarization buildup curves for all five carbon resonances were analyzed and fitted using both single-exponential (left) and biexponential (right) models. The fits clearly indicate biexponential behavior across all five resonances of proline. Note that again contributions of glycerol can be found as already shown in Figure 5. Details about the experimental data underlying this study are provided in the Supporting Information and data are available at Zenodo (https://zenodo.org/records/24086268).**

https://doi.org/10.5194/mr-2026-12
Preprint. Discussion started: 24 November 2026
© Author(s) 2026. CC BY 4.0 License.

Open Access MAGNETIC RESONANCE Discussions

## 3 Conclusion and outlook

Here, we have presented a complete workflow for acquiring SCREAM-DNP data, followed by post-processing and polarization buildup dynamic analysis. Therefore, we have introduced a Python package designed to fully automate the analysis of SCREAM-DNP datasets, with modular architecture that supports future expansion based on user requirements. The spectral deconvolution component could be extended to accommodate more complex spectral lineshapes, such as sideband patterns arising from chemical shift anisotropy under magic-angle spinning NMR. The buildup time analysis framework may similarly be expanded to incorporate simulations based on stretched exponential models, triexponential models, or linear buildup behavior. Additionally, the project could be generalized to function as a broader buildup/relaxation dynamics analyzer by implementing multiple importers capable of handling alternative experimental formats, such as vdlist-based pseudo-2D saturation recovery experiments. The latter is already implemented partially and may be used but has not been rigorously tested at the current state of the package. Further methods to reduce computational time while fitting, however, are also planned to be implemented. More information regarding this can be found online on https://screamlab.readthedocs.io/en/latest/. In all cases, the framework ensures fully reproducible and standardized data analysis in agreement with the FAIR principles.

## Code and data availability

Supporting information with test datasets as well as python scripts and further examples are available at Zenodo (https://zenodo.org/records/24086268).

## Supplement

The Supplement is available at Zenodo under the DOI 10.5281/zenodo.24086267.

## Author contributions

FPT implemented the SCREAMLAB software package and drafted the manuscript. ThB implemented the “scream.py” script for TopSpin. MS and TiB supported the programming and software architecture as well as aided with the publication and distribution of SCREAMLAB. EB performed extensive testing of SCREAMLAB and provided feedback and suggestions for additional functionality. BC supervised the project. All authors contributed to the drafting and revision of the manuscript.

## Competing interests

The author has declared that there are no competing interests.

https://doi.org/10.5194/mr-2026-12
Preprint. Discussion started: 24 November 2026
© Author(s) 2026. CC BY 4.0 License.



Open Access MAGNETIC RESONANCE Discussions

## Disclaimer

Publisher's note: Copernicus Publications remains neutral with regard to jurisdictional claims made in the text, published maps, institutional affiliations, or any other geographical representation in this paper. While Copernicus Publications makes every effort to include appropriate place names, the final responsibility lies with the authors. Views expressed in the text are those of the authors and do not necessarily reflect the views of the publisher.

## Financial support

This work was financially supported by the Deutsche Forschungsgemeinschaft (DFG) through the transregional collaborative research center TRR-386 (HYP*MOL: Hyperpolarization in molecular systems), projects A2 and A5, project number 514664767. The DNP upgrade was funded by the DFG through large instrument grant INST 264/177-1 FUGG, project number 438774970.

## References

Aladin, V. and Corzilius, B.: Methyl dynamics in amino acids modulate heteronuclear cross relaxation in the solid state under MAS DNP, Solid State Nuclear Magnetic Resonance, 99, 27–35, https://doi.org/10.1016/j.ssnmr.2019.02.004, 2019.

Aladin, V., Vogel, M., Binder, R., Burghardt, I., Suess, B., and Corzilius, B.: Complex Formation of the Tetracycline-Binding Aptamer Investigated by Specific Cross-Relaxation under DNP, Angewandte Chemie International Edition, 58, 4863–4868, https://doi.org/10.1002/anie.201811941, 2019.

Aladin, V., Sreemantula, A. K., Biedenbänder, T., Marchanka, A., and Corzilius, B.: Specific Signal Enhancement on an RNA-Protein Interface by Dynamic Nuclear Polarization, Chemistry – A European Journal, 29, e202203443, https://doi.org/10.1002/chem.202203443, 2023.

Biedenbänder, T., Aladin, V., Saeidpour, S., and Corzilius, B.: Dynamic Nuclear Polarization for Sensitivity Enhancement in Biomolecular Solid-State NMR, Chem. Rev., 122, 9738–9794, https://doi.org/10.1021/acs.chemrev.1c00776, 2022.

Biedenbänder, T., Bensons, E. R., and Corzilius, B.: Serial Polarization Transfer by Combination of Cross-Relaxation and Rotational Resonance for Sensitivity-Enhanced Solid-State NMR, ChemPhysChem, 24, e202300206, https://doi.org/10.1002/cphc.202300206, 2023.

Biskup, T.: Softwareentwicklung für die Naturwissenschaften: Bausteine computergestützter Datenauswertung, die den Ansprüchen der Wissenschaft gerecht wird, Springer, Berlin, Heidelberg, https://doi.org/10.1007/978-3-662-71607-6, 2026.

https://doi.org/10.5194/mr-2026-12
Preprint. Discussion started: 24 November 2026
© Author(s) 2026. CC BY 4.0 License.



Open Access MAGNETIC RESONANCE Discussions

Busch, H., Yasir Ateeque, M., Taube, F., Wiegand, T., Corzilius, B., and Künze, G.: Probing Biomolecular Interactions with Paramagnetic Nuclear Magnetic Resonance Spectroscopy, ChemBioChem, 26, e202400903, https://doi.org/10.1002/cbic.202400903, 2025.

Chow, W. Y., De Paëpe, G., and Hediger, S.: Biomolecular and Biological Applications of Solid-State NMR with Dynamic Nuclear Polarization Enhancement, Chem. Rev., 122, 9795–9847, https://doi.org/10.1021/acs.chemrev.1c01043, 2022.

van der Cruijsen, E. A. W., Koers, E. J., Sauvée, C., Hulse, R. E., Weingarth, M., Ouari, O., Perozo, E., Tordo, P., and Baldus, M.: Biomolecular DNP-Supported NMR Spectroscopy using Site-Directed Spin Labeling, Chemistry – A European Journal, 21, 12971–12977, https://doi.org/10.1002/chem.201501376, 2015.

Daube, D., Aladin, V., Heiliger, J., Wittmann, J. J., Barthelmes, D., Bengs, C., Schwalbe, H., and Corzilius, B.: Heteronuclear Cross-Relaxation under Solid-State Dynamic Nuclear Polarization, J. Am. Chem. Soc., 138, 16572–16575, https://doi.org/10.1021/jacs.6b08683, 2016.

Daube, D., Vogel, M., Suess, B., and Corzilius, B.: Dynamic nuclear polarization on a hybridized hammerhead ribozyme: An explorative study of RNA folding and direct DNP with a paramagnetic metal ion cofactor, Solid State Nuclear Magnetic Resonance, 101, 21–30, https://doi.org/10.1016/j.ssnmr.2019.04.005, 2019.

Goldfarb, D.: Gd3+ spin labeling for distance measurements by pulse EPR spectroscopy, Phys. Chem. Chem. Phys., 16, 9685–9699, https://doi.org/10.1039/C3CP53822B, 2014.

Good, D. B., Voinov, M. A., Bolton, D., Ward, M. E., Sergeyev, I. V., Caporini, M., Scheffer, P., Lo, A., Rosay, M., Marek, A., Brown, L. S., Smirnov, A. I., and Ladizhansky, V.: A biradical-tagged phospholipid as a polarizing agent for solid-state MAS Dynamic Nuclear Polarization NMR of membrane proteins, Solid State Nucl Magn Reson, 100, 92–101, https://doi.org/10.1016/j.ssnmr.2019.04.003, 2019.

Heiliger, J., Matzel, T., Can Çetiner, E., Schwalbe, H., Kuenze, G., and Corzilius, B.: Site-specific dynamic nuclear polarization in a Gd( iii )-labeled protein, Physical Chemistry Chemical Physics, 22, 25455–25466, https://doi.org/10.1039/D0CP05021K, 2020.

Helmus, J. J. and Jaroniec, C. P.: Nmrglue: an open source Python package for the analysis of multidimensional NMR data, J Biomol NMR, 55, 355–367, https://doi.org/10.1007/s10858-013-9718-x, 2013.

Herr, K., Fleckenstein, M., Brodrecht, M., Höfler, M. V., Heise, H., Aussenac, F., Gutmann, T., Reggelin, M., and Buntkowsky, G.: A novel strategy for site selective spin-labeling to investigate bioactive entities by DNP and EPR spectroscopy, Sci Rep, 11, 13714, https://doi.org/10.1038/s41598-021-92975-6, 2021.

Hoffmann, M. M., Bothe, S., Gutmann, T., and Buntkowsky, G.: Unusual Local Molecular Motions in the Solid State Detected by Dynamic Nuclear Polarization Enhanced NMR Spectroscopy, J. Phys. Chem. C, 121, 22948–22957, https://doi.org/10.1021/acs.jpcc.7b07965, 2017.

Kaushik, M., Bahrenberg, T., Can, T. V., Caporini, M. A., Silvers, R., Heiliger, J., Smith, A. A., Schwalbe, H., Griffin, R. G., and Corzilius, B.: Gd( III ) and Mn( II ) complexes for dynamic nuclear polarization: small

https://doi.org/10.5194/mr-2026-12
Preprint. Discussion started: 24 November 2026
© Author(s) 2026. CC BY 4.0 License.



Open Access MAGNETIC RESONANCE Discussions

molecular chelate polarizing agents and applications with site-directed spin labeling of proteins, Phys. Chem. Chem. Phys., 18, 27205–27218, https://doi.org/10.1039/C6CP04623A, 2016.

Klug, C. S. and Feix, J. B.: Methods and Applications of Site-Directed Spin Labeling EPR Spectroscopy, in: Methods in Cell Biology, vol. 84, Academic Press, 617–658, https://doi.org/10.1016/S0091-679X(07)84020-9, 2008.

Lafage, R., tisimst, Sjögren, R., mwang, Vidner, O., Antoine-Averland, Valle, E., Andrei, Schueller, J., Dietrich, J., Becker, M. R., Todd, and Fehlner, A.: pyDOE3: Design of experiments for Python (v1.0.2), https://doi.org/10.5281/zenodo.10958493, 2023.

Langa, Ł.: Black: The uncompromising Python code formatter, https://github.com/psf/black, 2018.

Lilly Thankamony, A. S., Wittmann, J. J., Kaushik, M., and Corzilius, B.: Dynamic nuclear polarization for sensitivity enhancement in modern solid-state NMR, Progress in Nuclear Magnetic Resonance Spectroscopy, 102–103, 120–195, https://doi.org/10.1016/j.pnmrs.2017.06.002, 2017.

Mao, J., Aladin, V., Jin, X., Leeder, A. J., Brown, L. J., Brown, R. C. D., He, X., Corzilius, B., and Glaubitz, C.: Exploring Protein Structures by DNP-Enhanced Methyl Solid-State NMR Spectroscopy, J. Am. Chem. Soc., 141, 19888–19901, https://doi.org/10.1021/jacs.9b11195, 2019.

Marin-Montesinos, I., Goyard, D., Gillon, E., Renaudet, O., Imberty, A., Hediger, S., and Paëpe, G. D.: Selective high-resolution DNP-enhanced NMR of biomolecular binding sites, Chemical Science, 10, 3366–3374, https://doi.org/10.1039/C8SC05696J, 2019.

McKay, M. D., Beckman, R. J., and Conover, W. J.: A Comparison of Three Methods for Selecting Values of Input Variables in the Analysis of Output from a Computer Code, Technometrics, 21, 239–245, https://doi.org/10.2307/1268522, 1979.

Newville, M., Stensitzki, T., Allen, D. B., and Ingargiola, A.: LMFIT: Non-Linear Least-Square Minimization and Curve-Fitting for Python (0.8.0), https://doi.org/10.5281/zenodo.11813, 2014.

Olver, F. W. J., Olde Daalhuis, A. B., Lozier, D. W., Schneider, B. I., Boisvert, R. F., Clark, C. W., Miller, B. V., and Saunders, B. C.: NIST Digital Library of Mathematical Functions, 2026.

Park, H., Uluca-Yazgi, B., Heumann, S., Schlögl, R., Granwehr, J., Heise, H., and Schleker, P. P. M.: Heteronuclear cross-relaxation effect modulated by the dynamics of N-functional groups in the solid state under 15N DP-MAS DNP, Journal of Magnetic Resonance, 312, 106688, https://doi.org/10.1016/j.jmr.2020.106688, 2020.

Prospector Development Team: Prospector: Inspects Python source files, https://github.com/prospector-dev/prospector, n.d.

Rogawski, R., Sergeyev, I. V., Li, Y., Ottaviani, M. F., Cornish, V., and McDermott, A. E.: Dynamic Nuclear Polarization Signal Enhancement with High-Affinity Biradical Tags, J. Phys. Chem. B, 121, 1169–1175, https://doi.org/10.1021/acs.jpcb.6b09021, 2017.

https://doi.org/10.5194/mr-2026-12
Preprint. Discussion started: 24 November 2026
© Author(s) 2026. CC BY 4.0 License.



Open Access MAGNETIC RESONANCE Discussions

Smith, A. N., Caporini, M. A., Fanucci, G. E., and Long, J. R.: A method for dynamic nuclear polarization enhancement of membrane proteins, Angew Chem Int Ed Engl, 54, 1542–1546, https://doi.org/10.1002/anie.201410249, 2015.

Sphinx Development Team: Sphinx Documentation, 2026.

Taube, F.: screamlab, https://doi.org/10.5281/zenodo.16748661, 2026.

Taube, F., Gierth, M., Künze, G., and Corzilius, B.: Proline Ring-Inversion Dynamics in Peptides Enable Cross-Relaxation-Based Dynamic Nuclear Polarization, Chemphyschem, 27, e70444, https://doi.org/10.1002/cphc.70444, 2026.

Viennet, T., Viegas, A., Kuepper, A., Arens, S., Gelev, V., Petrov, O., Grossmann, T. N., Heise, H., and Etzkorn, M.: Selective Protein Hyperpolarization in Cell Lysates Using Targeted Dynamic Nuclear Polarization, Angewandte Chemie, 128, 10904–10908, https://doi.org/10.1002/ange.201603205, 2016.

Voinov, M. A., Good, D. B., Ward, M. E., Milikisiyants, S., Marek, A., Caporini, M. A., Rosay, M., Munro, R. A., Ljumovic, M., Brown, L. S., Ladizhansky, V., and Smirnov, A. I.: Cysteine-Specific Labeling of Proteins with a Nitroxide Biradical for Dynamic Nuclear Polarization NMR, J. Phys. Chem. B, 119, 10180–10190, https://doi.org/10.1021/acs.jpcb.5b05230, 2015.

Wilkinson, M. D., Dumontier, M., Aalbersberg, Ij. J., Appleton, G., Axton, M., Baak, A., Blomberg, N., Boiten, J.-W., da Silva Santos, L. B., Bourne, P. E., Bouwman, J., Brookes, A. J., Clark, T., Crosas, M., Dillo, I., Dumon, O., Edmunds, S., Evelo, C. T., Finkers, R., Gonzalez-Beltran, A., Gray, A. J. G., Groth, P., Goble, C., Grethe, J. S., Heringa, J., 't Hoen, P. A. C., Hooft, R., Kuhn, T., Kok, R., Kok, J., Lusher, S. J., Martone, M. E., Mons, A., Packer, A. L., Persson, B., Rocca-Serra, P., Roos, M., van Schaik, R., Sansone, S.-A., Schultes, E., Sengstag, T., Slater, T., Strawn, G., Swertz, M. A., Thompson, M., van der Lei, J., van Mulligen, E., Velterop, J., Waagmeester, A., Wittenburg, P., Wolstencroft, K., Zhao, J., and Mons, B.: The FAIR Guiding Principles for scientific data management and stewardship, Sci Data, 3, 160018, https://doi.org/10.1038/sdata.2016.18, 2016.